Nuclear Inst. and Methods in Physics Research, A 1039 (2022) 166994

Contents lists available at ScienceDirect

Nuclear Inst. and Methods in Physics Research, A

journal homepage: www.elsevier.com/locate/nima

Optimal injection voltage in the LHC

L. Medina *, H. Timko, T. Argyropoulos, E. Shaposhnikova, B. Salvachua, J. Wenninger, I. Karpov, P. Baudrenghien, M. Palm

CERN, CH-1211, Geneva 23, Switzerland

ARTICLE INFO

Keywords:
Synchrotron
Beam injection
Bunch-to-bucket transfer

ABSTRACT

Finding the optimal rf injection voltage in the LHC is a trade-off between minimising capture and flat-bottom losses, which call for an increased voltage, and minimising rf power consumption as well as improving beam stability, both of which call for a reduced voltage. From the beam stability point of view, earlier particle-tracking simulations showed that the decrease of the injection voltage from 6 MV to 4 MV is beneficial. This reduction was performed in the LHC Run 2 over a three-week period in steps of 0.5 MV. The impact of different voltages and injection energy errors on the evolution of beam parameters such as bunch length and beam losses are analysed in this paper. Operation at 4 MV, maintained in the machine after the reduction period, is studied in more detail. The implications for the future High-Luminosity LHC operation with high-intensity beams are also discussed.

1. Introduction

In the LHC Design Report [1], the maximum 400 MHz rf voltage at the 450 GeV injection energy was originally foreseen to be 8 MV [2,3]. This value, which is much higher than the matched voltage, would allow accommodating for the largest possible bunch emittance injected with the expected rf phase and energy errors. At that time, the SPS (the LHC injector) was operated with the Q26 optics and a transition gamma of $\gamma_t = 22.83$, producing the 25 ns standard beam (four batches of 72 bunches spaced at 25 ns) with relatively large longitudinal emittance. The SPS main rf system operates at 200 MHz and, with its bucket length being twice as large as that of the LHC, the bunches produced in the SPS can have long tails. Upon the first beam commissioning in the LHC, attempts were made to use a voltage of around 3 MV, which is much closer to the matched voltage; this, however, led to significant capture losses. With the SPS Q26 optics, the LHC injection voltage was later optimised experimentally to 6 MV. In LHC Run 2 (2015–2018), the proton beams were accelerated in the SPS with the Q20 optics ($\gamma_t = 18.0$). This, together with the change of the beam production scheme from the standard to the batch compression, merging, and splitting (BCMS) scheme [4] in the PS (the injector of the SPS), resulted in smaller transverse and longitudinal emittances at LHC injection.

Although the two machines do not have the same bucket length, the *matched* voltage in the LHC can be obtained assuming the same bunch length $\tau_{\mathrm{SPS}} = \tau_{\mathrm{LHC}}$ and the same corresponding longitudinal emittance $\epsilon_{\mathrm{SPS}} = \epsilon_{\mathrm{LHC}}$ in both machines. Neglecting the effect of the fourth-harmonic Landau cavity in the SPS, the emittance in a single-harmonic rf system can be calculated as

$$\epsilon = \frac{2Ef_{s,0}\beta^2}{\pi f_{\mathrm{rf}}^2 \eta_0} \int_0^{\varphi_b} d\varphi \sqrt{2(\cos\varphi - \cos\varphi_b)} \equiv \frac{2Ef_{s,0}\beta^2}{\pi f_{\mathrm{rf}}^2 \eta_0} I\,, \tag{1}$$

where E is the synchronous kinetic energy, $f_{s,0}$ the central synchrotron frequency, β the relativistic beta, η_0 the zeroth-order slippage factor, f_{rf} the rf frequency, and $\varphi_b = \pi f_{\mathrm{rf}} \tau$ the amplitude of bunch phase oscillations corresponding to a given bunch length. The matched voltage in the LHC can then be calculated as

$$V_{\mathrm{LHC}} = \frac{h_{\mathrm{LHC}}^3 f_{\mathrm{rev,LHC}}^2 \eta_{0,\mathrm{LHC}}}{h_{\mathrm{SPS}}^3 f_{\mathrm{rev,SPS}}^2 \eta_{0,\mathrm{SPS}}} \frac{I_{\mathrm{SPS}}^2}{I_{\mathrm{LHC}}^2} V_{\mathrm{SPS}}\,. \tag{2}$$

Using the parameters in Table 1 and assuming a bunch length of 1.45 ns, the matched voltage in the LHC would be 2.0 MV.

Long-lasting bunch phase oscillations after injection were observed since the start-up of the LHC but were not considered to be harmful. Often referred to as *dancing bunches*, these oscillations were also observed in other machines, such as the Tevatron [5], RHIC, and SPS, and can lead to instabilities [6]. Undamped bunch oscillations in the LHC are the result of the loss of Landau damping at the operational beam parameters [7]. These oscillations were effectively suppressed in the Tevatron using a longitudinal damper, and an alternative method was proposed and tested [8]. In the LHC, experimental studies of bunch phase oscillations after beam capture restarted [9] as they were seen to survive the controlled longitudinal emittance blow-up during the acceleration ramp [10], potentially affecting the quality of the future high-intensity beams for physics. Additionally, undamped oscillations

* Corresponding author.
E-mail addresses: medinamluis@gmail.com (L. Medina), helga.timko@cern.ch (H. Timko).

https://doi.org/10.1016/j.nima.2022.166994
Received 25 January 2022; Received in revised form 24 April 2022; Accepted 24 May 2022
Available online 18 June 2022
0168-9002/© 2022 The Author(s). Published by Elsevier B.V. This is an open access article under the CC BY license (http://creativecommons.org/licenses/by/4.0/).

Table 1
LHC and SPS machine-dependent parameters during the reduction campaign of the LHC injection voltage in Run 2.

Parameter	SPS value	LHC value
Harmonic number	4620	35 640
Revolution frequency	43 375 Hz	11 245 Hz
Relativistic γ at transition	18.0	53.8
Zeroth-order slippage factor	3.08×10^{-3}	3.41×10^{-4}
Number of bunches	96 or 144	2556
Main rf voltage	7 MV	6 MV → 4 MV
Fourth harmonic rf voltage (bunch-shortening mode)	1.24 MV	

in beam tests with intensities approaching the High-Luminosity LHC (HL-LHC) target led to non-negligible particle losses during the time spent at flat-bottom. In simulations, the large mismatch between the rf bucket and the injected bunch shape in the longitudinal phase space was found to lead to the observed undamped injection oscillations in the presence of injection errors in phase and/or energy, and intensity effects [11]. Demonstrated by these simulations, the optimum injection voltage is thus a trade-off between two effects: while a reduced injection (or capture) voltage results in a smaller bucket and better matching and beam stability, an increased voltage yields a larger bucket height, hence minimising capture losses.

Moreover, a low injection voltage is also desirable to reduce rf power consumption in the coming LHC Run 3 and HL-LHC with the planned double beam intensities. To assess possible power limitations, the present rf power availability in the LHC has been probed in beam measurements [12]. The rf power consumption increases at higher intensities due to strong beam-loading [13,14]. Reducing the rf voltage helps reduce the power consumption by decreasing the beam-induced component of the total induced voltage in the rf cavities [15]. First, simplified simulation studies have been performed to estimate whether the presently available rf power will be sufficient for the targeted beam intensity and increased bunch momentum spread at LHC injection [16–18]. However, addressing this issue in simulations is a complex undertaking, as it requires detailed modelling of intensity effects, beam losses at LHC capture and along the flat-bottom, and an accurate bunch distribution generation in the SPS. All this requires building custom models of beam- and cavity control loops in both the LHC and the SPS, which is currently ongoing. As a crucial part of these power limitation studies, the minimum voltage required for the future operation of the LHC machine has to be assessed using the analysis of the present situation.

In Section 2 of this paper, the previous work on energy matching, beam-loading compensation, and single-bunch oscillations at injection is summarised. Section 3 presents the results of the voltage reduction campaign in the LHC, discussing the measurements of bunch length, losses, and satellite population. Section 4 analyses the energy errors at injection and their damping. The injection voltage and power requirements for the HL-LHC are reviewed in Section 5. Lastly, studies and improvements planned for the future are discussed in Section 6.

2. Previous studies

2.1. SPS-LHC energy matching

A good energy matching between the SPS and the LHC is crucial when transferring the beam from the 200 MHz main rf system of the SPS to the half-as-long buckets of the LHC. The calibration and the long-term stability of the beam energy at SPS extraction were studied extensively during the construction of the LHC [19,20]. The original calibration of the SPS dipole field with ion and low-intensity proton beams at 450 GeV showed a reproducibility of 10^{-4} in the relative momentum offset, over the timescale of months. This corresponds to an energy offset of 45 MeV, while the LHC bucket height is ±(318–390) MeV for injection voltages of 4 MV to 6 MV.

2.2. RF power and beam-loading compensation

In the LHC, the beam-loading of high-intensity proton beams is responsible of a significant portion of the rf power consumption. The half-detuning beam-loading compensation scheme was proposed during the LHC rf design phase [13] and it is still the baseline scheme at injection for the HL-LHC. It minimises the peak rf power in static conditions by optimising the position of the cavity main power coupler and the frequency of the rf cavity detuning to correspond to a half of the peak rf beam current.

In the nominal LHC operational scheme with 1.15×10^{11} protons per bunch (p/b), the highest power consumption of 275 kW per cavity [1] would occur at flat-top when using the maximum voltage of 16 MV per beam (2 MV per cavity). The klystrons, feeding one rf cavity each, were therefore specified at 330 kW [21], allowing for a 20% power margin for the transients. Power saturation was observed in beam measurements at 250 kW – 280 kW [12], and optimisation to reach the design power limit is ongoing.

An alternative beam-loading compensation scheme called full detuning [14,22] is the baseline for the energy ramp and flat-top in the HL-LHC. It reduces the power consumption by allowing the rf phase to shift from one bunch to another, enabling the use of the same 16 MV total voltage with a bunch population of 2.3×10^{11} p/b. This scheme, however, cannot be applied at flat-bottom for the capture of equidistant bunches without significant emittance blow-up and losses. In addition, future high-intensity SPS beams will have a larger bunch emittance with similar bunch length (minimum possible with available SPS rf voltage), calling for larger injection voltages in the LHC.

2.3. Single-bunch undamped oscillations

Concerning undamped oscillations observed at LHC flat-bottom [9], first single-bunch simulations with the Beam Longitudinal Dynamics (BLonD) Simulation Suite [23,24] were performed during LHC Run 2. These studies showed that for high bunch intensities, the combination of injection errors (in phase and/or energy) and a mismatched bucket height lead to the creation of density islands in the longitudinal phase space and to persistent non-rigid dipole oscillations during the filamentation process after injection [11]. The measured peak-to-peak amplitude of these phase oscillations can be as large as 50°.

To determine the optimum machine configuration, beam losses at flat-bottom and oscillation amplitude were studied as a function of the bunch length and injection voltage. An LHC injection voltage of 4 MV was found to be a good compromise between reduced losses and a reasonable stability margin, and was thus later targeted in machine operation. Once the minimum rf voltage V is found operationally for a given momentum spread δ and assuming perfect energy matching, we can use a simple scaling based on δ' to obtain the minimum voltage V' for other beam parameters,

$$V'_{\mathrm{LHC}} = \left(\frac{\delta'_{\mathrm{SPS}}}{\delta_{\mathrm{SPS}}} \right)^2 V_{\mathrm{LHC}} \,. \tag{3}$$

The above formula also confirms that the original LHC operational voltage of 6 MV was indeed the minimum voltage for beams produced in the SPS with the Q26 optics in the past. In the absence of more simulation studies, this formula also provides the best voltage estimates needed for Run 3 and the HL-LHC.

3. Voltage reduction campaign

The rf voltage at injection in the LHC was progressively reduced from 6 MV to 4 MV in steps of 0.5 MV over a period of roughly one month (LHC fills 7035 to 7110) to collect and compare fill-to-fill data. The effect of the voltage amplitude on various beam parameters is discussed in detail in the present section. The relevant operational parameters of both the LHC and the SPS during the LHC injection voltage reduction campaign are shown in Tables 1 and 2.

Table 2
Beam parameters during the reduction campaign of the LHC injection voltage in Run 2.

Parameter	Value
Momentum	450 GeV/c
Average bunch length at SPS extraction	(1.42 – 1.48) ns
Bunch intensity (protons) at LHC injection	(1.05 – 1.10)×10^{11} p/b

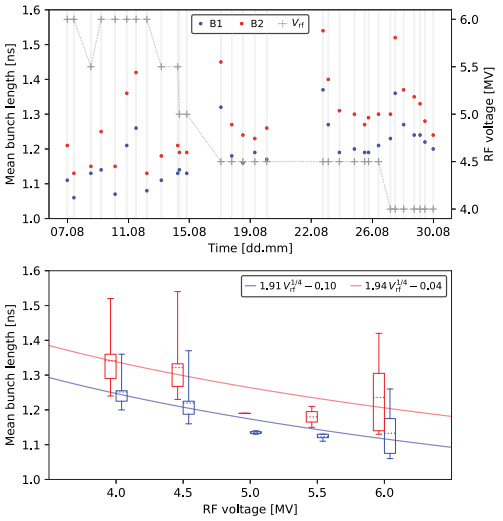

Fig. 1. Evolution of the mean bunch length (average over the full beam) at the start of the ramp of each fill of the rf voltage reduction campaign (*top*), and corresponding distribution as a function of the operated injection voltages (*bottom*). For each beam and voltage, each box contains half of the measurements, the inner dashed line indicates the average, and the whiskers display the peak-to-peak range of the measurements. In the bottom plot, the solid lines correspond to fits $\tau \propto V^{-1/4}$, as expected from synchrotron motion.

3.1. Bunch length

In all measurement and simulation results presented in this paper, the bunch length is defined as a scaled full width half maximum (FWHM) bunch length,

$$\tau \equiv \frac{2}{\sqrt{2\ln 2}}\mathrm{FWHM}\,. \tag{4}$$

For a Gaussian bunch, this results in a 4σ-bunch length.

A large fill-to-fill variation of the mean bunch length (average over the full beam and measured at the start of the ramp) is observed (Fig. 1, top). Note that, for the 5.0 MV and 5.5 MV cases, there is not much statistics and therefore the error bars are underestimated. With no additional blow-up, the filamented bunch lengths τ scale with the injection voltage V as expected, i.e. $\tau \propto V^{-1/4}$, as seen on the bottom plot. The bunch length was found to remain 0.1 ns larger on average for beam 2 (B2) than for beam 1 (B1) throughout the full voltage reduction campaign. This asymmetry points to a systematic blow-up of B2 with respect to B1, since the beam quality at LHC injection is, in principle, the same for both beams independently of the ring into which they are injected. Ideally, this difference should be reduced to the minimum to mitigate any impact on the physics operation of the machine. At the moment, there is no previous experience with this asymmetry, which only seems to have been made evident by the lower injection voltage. With the LHC currently restarting Run 3, the source of this asymmetry is expected to be determined and corrected in the upcoming operation.

3.2. Beam losses

The longitudinal beam losses originate mainly from the beam halo. Two types of losses are studied, namely, capture and flat-bottom losses.

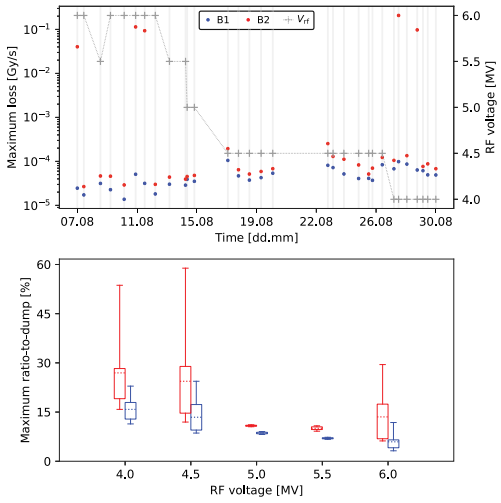

Fig. 2. Evolution of the maximum losses (*top*) at the start of the ramp of each fill of the rf voltage reduction campaign, and corresponding ratio-to-dump as a function of the operated injection voltages (*bottom*). The box parameters are defined as in Fig. 1.

Immediate capture losses occur at the bunch-to-bucket transfer between the SPS and LHC. Large phase and energy injection errors, as well as large beam halo population enhance capture losses. Flat-bottom losses occur as halo particles slowly leak out of the bucket due to rf noise and intrabeam scattering (IBS), and their magnitude depends on the time spent at injection energy. While a lower rf voltage leads to a smaller bucket area and increases the capture losses, it also yields a slightly reduced blow-up from filamentation due to the smaller mismatch. The reduced longitudinal emittance, however, leads to stronger IBS if the injection errors are small. Thus, both capture and flat-bottom losses are expected to increase as the injection voltage decreases. A large injection voltage, on the other hand, can lead to long-lasting injection oscillations which can also be accompanied by significant flat-bottom losses [9].

In operation, the two types of losses cannot be easily distinguished. Their sum is normally seen at the start of the ramp as a momentary drop in beam intensity (or a spike in measured beam losses) lasting a short period. If a beam dump occurs due to large start-of-ramp losses, it results in at least a two-hours loss of physics production due to the slow cycling of the superconducting magnets of the LHC. To maintain good machine availability, beam losses at the start of the ramp should therefore be kept below the dump thresholds that are in place to protect sensitive equipment.

The LHC beam loss monitors of the BLMI-type [25,26] consist of ionisation chambers of about 50 cm, located around the machine in positions where beam losses are expected. They provide beam loss measurements with twelve different integration times (or running sums), for which different beam dump thresholds apply. The top plot of Fig. 2 shows the recorded maximum losses among all running sums of all BLMIs at the start of the ramp of each physics fill during the voltage reduction campaign. The ratio-to-dump $r_{i,\mathrm{RS}}$ is defined as the ratio between the beam loss $L_{i,\mathrm{RS}}$ measured by a monitor i with a given running sum RS and its corresponding dump threshold $\mathrm{T}_{i,\mathrm{RS}}$,

$$r_{i,\mathrm{RS}} \equiv \frac{L_{i,\mathrm{RS}}}{T_{i,\mathrm{RS}}}\,. \tag{5}$$

The bottom plot shows the distribution of the maximum ratio-to-dump among all monitors and all their running sums, as a function of the different injection voltages.

As the voltage is reduced from 6 MV to 4 MV, both the fill-to-fill average losses and the maximum losses increase. In most cases, the largest losses in the ring occurred around the location of the off-momentum collimators (LHC Point 3) and, to a lesser extent, at the

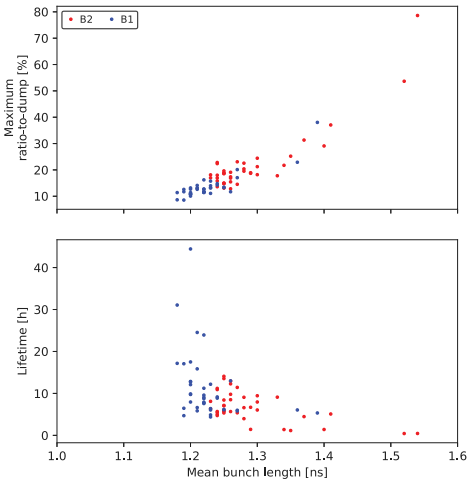

Fig. 3. Maximum ratio-to-dump (*top*) at the start of the ramp and corresponding instantaneous beam lifetime (*bottom*) as a function of the mean bunch length (average over the full beam) of each fill with an injection voltage of 4 MV. For a given monitor and running sum, the ratio-to-dump is defined as the ratio between the measured beam loss and its corresponding dump threshold. The instantaneous beam lifetime is derived from the *instantaneous* decrease rate of the beam intensity at the time of the maximum losses.

location of the betatron collimators (LHC Point 7). Similarly to the mean bunch length measurements, the maximum losses (and the corresponding maximum ratio-to-dump) remain consistently larger for B2 than for B1. Although no beam dumps occurred at low voltage during the two months of proton operation, several B2 fills reached 60 % of the dump threshold. While this was not an issue in the 2018 operation thanks to the small injected emittances and stable beam parameters, the beam quality might be worse after the Long Shutdown 2 (LS2) due to higher beam intensities, and beam dumps due to losses could affect machine availability.

Whenever a large energy mismatch between the SPS and LHC occurs, the injected bunches are blown up and the losses increase. In the LHC, there is no batch-by-batch damper to correct injection errors. The fills where the ratio-to-dump was higher than average correspond to fills with a large energy mismatch between the two machines and, as a consequence, with large longitudinal emittance blow-up. Therefore, to maintain high machine availability in the future, an improved SPS-LHC energy matching and a review of the current LHC dump thresholds are important, both being currently under investigation.

The momentary rise of the losses at the start of the ramp is also seen as a reduction of the beam lifetime for a short period. The minimum lifetime dt is derived from the *instantaneous* decrease of the beam intensity dI at the time of the maximum loss rate (dI/dt), i.e.

$$dt = \frac{dI}{dI/dt}\,. \tag{6}$$

The estimated lifetime is shown in Fig. 3 for physics fills operated with the reduced injection voltage of 4 MV. As expected, higher losses and a reduced beam lifetime are correlated with the bunch length.

3.3. Satellite and ghost population

Particles lost from the main bunches due to injection errors, IBS, rf noise, etc., can get recaptured at the start of the acceleration ramp into the empty buckets. In the LHC, the lost particles located within a 25 ns-window around the main bunches are called *satellite* population, while those located beyond this range constitute the *ghost* population [27]. Since collisions are processed by the LHC detectors at a rate of 40 MS/s, main-bunch data cannot be distinguished from satellite data. As a consequence, the satellite population is required by the experiments

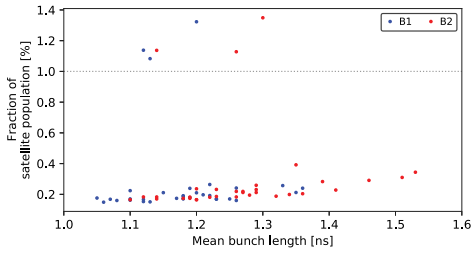

Fig. 4. Satellite population as a function of the mean bunch length (average over the full beam) at the start of the ramp of each fill of the rf voltage reduction campaign. The satellite population is defined as the lost particles located within a 25 ns-window around the main bunches.

to remain below 1 % in physics fills to keep the background noise in collision data below an acceptable limit.

Flat-bottom losses in the LHC are not the only source of satellite and ghost particles. Satellites are also created and preserved in the injector chain of the LHC. Circulating in the 40 MHz rf buckets of the PS, the 25 ns bunch trains are shortened via bunch rotation before their extraction. This rotation in phase space results in uncaptured halo particles at injection into the SPS 200 MHz buckets; part of them is then recaptured at the start of the SPS acceleration ramp in the neighbouring buckets.

As the bunch length increased with a reduced LHC injection voltage, measurements showed a slight increase in the satellite and ghost populations. Since the ghost population is around one order of magnitude lower than the satellite population and therefore not critical for the experimental data quality, the following analysis focuses only on the latter. Fig. 4 shows the start-of-ramp satellite population of the fills of the voltage reduction campaign. As observed, it remained far below the 1% threshold, except for a few cases, with only a weak dependence on the rf voltage. In fact, transfer losses between the PS and the SPS had a larger impact on the LHC satellite population than the LHC injection voltage. All fills with a satellite population above 1% actually correspond to fills where the PS bunch rotation was not optimal. The largest recorded satellite population of around 1.4% corresponds, for example, to fill 7083 in which one of the two 40 MHz PS cavities used for bunch rotation was not operational. While the satellite population is preserved throughout the ramp, it does not pose an issue at flat-top.

4. Injection errors and SPS-LHC energy matching

4.1. Fill-by-fill evolution

The relative momentum offset between the SPS and the LHC was computed from the first-turn trajectory in the first arc of the LHC, for fills with an rf voltage of 4 MV. The momentum error is obtained by fitting the injection trajectory to a betatron oscillation with dispersive component due to an energy error; no corrections from variations of the rf frequency or tides are necessary for first-turn measurements. As seen in the top plot of Fig. 5, the injection errors (in parts-per-million or ppm, i.e. 10^{-6}) exhibit a large spread from fill to fill. Only nominal intensity bunches were considered (no low-intensity pilots), and the last injections were systematically omitted due to an acquisition trigger problem of the Beam Position Monitor (BPM) system.

The mean bunch length per fill (average over the full beam) at the start of the ramp is shown in the bottom plot of Fig. 5 as a function of relative momentum offset per injection. Determined by the filamentation process after injection, the average bunch length is observed to follow the same dependency with respect to the injection errors for both beams. The lowest bunch length is expected to represent a perfectly-matched beam transfer. Quadratic fits are shown in solid lines; they suggest that, while the measured zero momentum-offset indeed corresponds to perfect matching for B1, a systematic measurement

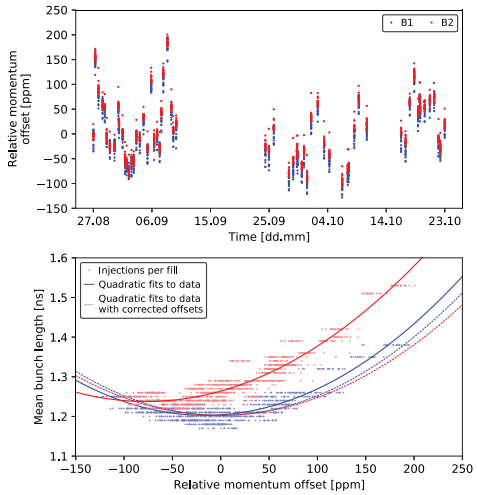

Fig. 5. Relative momentum offset (*top*) per injection and correlation with the mean bunch length (average over the full beam) at the start of the ramp (*bottom*). Data from fills with an injection voltage of 4 MV. In the bottom plot, the solid lines correspond to quadratic fits to highlight the trends of the measurements. These fits are shifted so that their vertex coincides with a zero momentum offset (dotted lines).

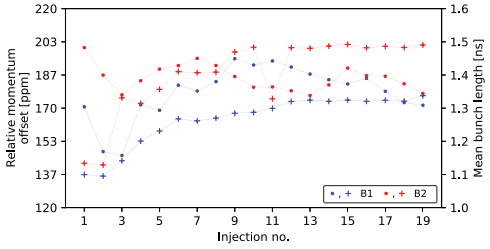

Fig. 6. Relative momentum offset (·) and mean bunch length (+, average over the injected batches) per injection from fill 7139. The first injection consists of a batch of 12 bunches; the sixth, eleventh, and sixteenth contain two batches of 48 bunches; and the remainder consist of three batches of 48 bunches.

error on the relative momentum offset of about −60 ppm seems to be present in B2. Furthermore, a systematic blow-up of about 35 ps can be observed in B2 with respect to B1 at perfect energy matching. As both beams arrive with the same beam quality (and thus bunch length, on average) from the SPS, this blow-up can only be attributed to the LHC, and its differences between Rings 1 and 2. The dashed lines in Fig. 5 show the corresponding B1 and B2 fits with both the momentum and bunch length offsets corrected.

Without a readjustment of the energy matching between the two machines over a period of a month, the mismatch can reach up to around 200 ppm. This value is twice the expected mismatch based on purely the SPS dipole field stability [20]. The spread from one injection to another within one fill is typically less than 50 ppm. The mismatch should be significantly reduced with a more frequent energy matching between the two machines. If the mismatch could be kept within ±50 ppm, the bunch length would virtually not be affected, as shown in Fig. 3, resulting in minimal beam losses.

4.2. Damping of injection errors

Injection oscillations are partially damped in phase and energy by the beam phase loop. In the LHC, the beam phase loop applies the necessary correction calculated using the average bunch phase of all circulating bunches [28]. Fig. 6 shows the momentum offset and mean bunch length per injection (average over the injected batches) from fill 7139, a fill with one of the largest measured momentum offsets. As seen in the plot, the beam phase loop effectively damps the first

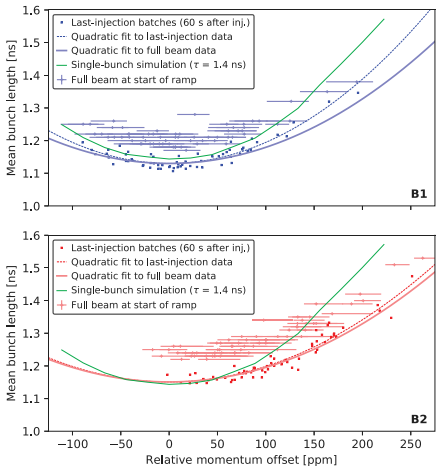

Fig. 7. Mean bunch length of the batches of the last injection (measured 60 s after injection to allow filamentation) as a function of the relative momentum offset at injection (dark points). Data from fills with an rf voltage of 4 MV for the B1 (*top*) and B2 (*bottom*). The mean bunch length of the full beam at the start of the ramp (light points with error bars) is included for comparison. The data is shifted so that the corresponding quadratic fits are centred around zero momentum offset; the fits of the full beam data (solid line) are shifted, additionally, in the vertical axis to directly compare with the fits of the last-injection data (dashed line). Results from a single-bunch simulation with a bunch length of $\tau = 1.4$ ns (green line) are included for comparison.

batches: blow-up is kept at a minimum, resulting in a lower average bunch length of the injected batches. The damping becomes less and less efficient with every new injection, and the mean bunch length grows. Moreover, each time a new batch injection with large phase or energy errors takes place, the circulating batches will all receive a non-negligible kick, which can lead to further blow-up.

Frequent energy matching between the SPS and the LHC can be time-consuming, thus affecting the machine efficiency. Additionally, it may be insufficient at low injection voltages, where more capture losses are produced, since it cannot correct the batch-by-batch energy errors. In this case, a longitudinal damper might be required for operation in the future. A longitudinal damper using the accelerating cavities themselves to damp dipole modes was in fact originally foreseen for the LHC, allowing the batch-by-batch damping of phase and energy errors at injection [1]. Up to now, this damper has not been needed and therefore has not been commissioned.

4.3. Bunch length and oscillation amplitude

Bunch length growth can be due to blow-up following injection errors or, at flat-bottom, due to rf noise and IBS. To separate these two effects, the mean bunch length of the batches of the last injection (at about 60 s after injection to allow filamentation) is compared with the average bunch length of the full beam at the start of the ramp. For the last injection, the batches remain virtually unaffected by the beam phase loop, and the phase noise and IBS can be neglected on this time scale. Measurements for both beams from physics fills with a 4 MV injection voltage are displayed in Fig. 7. Similarly to Fig. 5, quadratic fits for the bunch lengths as a function of the relative momentum offset are included. The systematic errors in both the data and the corresponding parabolic fits are compensated (i.e. the minimum of each data set and its parabolic fit are centred at zero momentum offset). The fits of the full beam data are shifted, additionally, in the vertical axis to directly compare with the fits of the last-injection data. The blow-up with large energy errors is found to be more pronounced on the last-injection measurements when compared with the full beam, especially for B1.

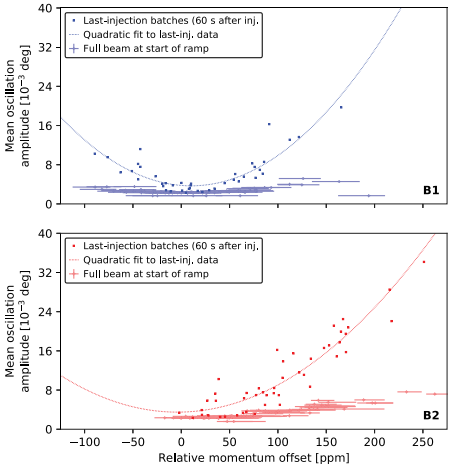

Fig. 8. Mean amplitude of phase oscillations of the batches of the last injection (measured 60 s after injection to allow filamentation) as a function of relative horizontal momentum offset at injection (dark points). Data from fills with an rf voltage of 4 MV for B1 (*top*) and B2 (*bottom*). The mean amplitude of phase oscillations of the full beam at the start of the ramp (light points with error bars) is included for comparison. The data points have been shifted in a similar way as in Fig. 7.

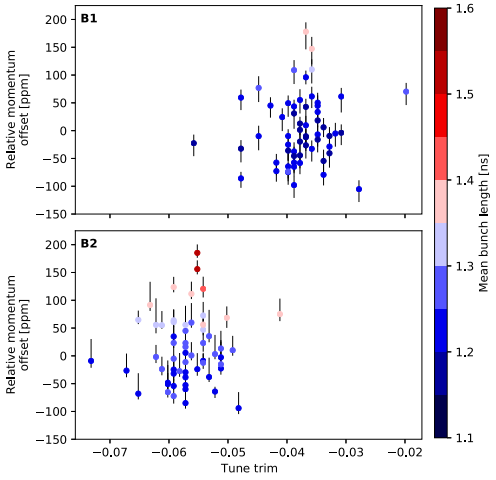

Fig. 9. Relative momentum offset per fill and corresponding manual tune trims. Data from fills with an rf voltage of 4 MV for B1 (*top*) and B2 (*bottom*). The central dot and the bars represent the average and the maximum/minimum momentum offsets over all the injections in the fill, respectively. The corresponding mean bunch length over the full beam at the start of the ramp is colour-coded.

To compare with these measurements, a first single-bunch tracking simulation was performed with BLonD assuming an SPS extraction bunch length of 1.4 ns. The green line in Fig. 7 shows the resulting filamented bunch length in the LHC as a function of the momentum mismatch. This simple model describes relatively well the behaviour of the last-injection bunches, but the discrepancy observed at large momentum offsets shows that more sophisticated simulations are required to describe the measurements in this regime. Indeed, a realistic modelling of the beam injection aiming at reproducing machine measurements must take into account accurate bunch distributions (especially for the population), multi-bunch batches, intensity effects, rf noise and control loops. Such simulations also have to be benchmarked with more accurate measurements of bunch parameters and injection errors which will only be available in the upcoming LHC Run 3, and for a wide range of operational conditions. This, however, goes beyond the scope of the present paper as it is an extensive ongoing work.

The dipole oscillation amplitude measurements as a function of the energy mismatch are shown in Fig. 8 for fills with an injection voltage of 4 MV. At a 200 ppm relative momentum offset, the mean oscillation amplitude of the last injected batches increases by a factor of about six with respect to the oscillations observed at perfect matching. Globally, it follows the same behaviour of the bunch length with the momentum offset. By the start of the ramp, the mean oscillation amplitude of the full beam is largely damped, although some excitation remains for large momentum offsets.

As the injection voltage is reduced, the amplitude of dipole oscillations is expected to decrease. This was indeed observed, with the mean oscillation amplitude with 6 MV injection voltage found to be $(3.2^{+3.9}_{-1.4}) \times 10^{-3}$ deg and $(4.5^{+3.0}_{-2.7}) \times 10^{-3}$ deg for B1 and B2, respectively, and decreasing to $(2.4^{+1.1}_{-0.1}) \times 10^{-3}$ deg and $(2.7^{+1.3}_{-0.5}) \times 10^{-3}$ deg, respectively at 4 MV (the $\pm$ values correspond to the offsets of the maximum and minimum measurement with respect to the average). From these figures, we can conclude that the fill-to-fill spread of the oscillation amplitudes also visibly decreases with the reduced injection voltage. While the reduction of bunch phase oscillations by means of the decrease of the injection voltage is a passive approach, the use of a longitudinal damper (provided enough rf power at injection is available) would allow to operate at a higher rf voltage and thus minimise injection losses.

4.4. SPS and LHC as potential sources of energy errors

In the LHC, transverse tune corrections are automatically applied at injection taking into account the persistent current field decay of the dipole and quadrupole magnets and the beam-intensity-dependent tune shifts. Nevertheless, unpredicted tune errors are observed from fill to fill at injection; they are corrected during adjustments of the (low-intensity) probe beam before proceeding to fill the machine with the nominal physics beam. There are many possible origins for those unpredicted tune errors, including an error on the main dipole field. A dipole field error in the LHC may generate a significant tune shift through the natural chromaticity of around −60 units.

A correlation between the energy offsets, determined from the first-turn data, and the manual tune trims (corrections) used to compensate for the unpredicted tune changes would point towards the LHC as a source of the energy errors at beam transfer between the SPS and LHC. Fig. 9 shows the fill-to-fill applied tune trims and relative momentum offset in both beams. The absence of a correlation lets us conclude that the primary source of the SPS-LHC energy mismatch is not the LHC dipole field. Those unpredicted LHC tune changes are therefore likely due to imperfections in the modelling of the quadrupolar component of the field decay and not to a dipole field variation.

5. Injection voltage and power requirements for the HL-LHC

A simple scaling using Eq. (3) with the minimum 4 MV injection voltage in the LHC and assuming the expected momentum spread of the arriving high-intensity bunches with the SPS voltage upgrade to 10 MV (in the Q20 optics) as well as an average bunch length of 1.50 ns to 1.65 ns at SPS extraction yields a minimum 7 MV to 8 MV injection voltage for the HL-LHC [29]. For the HL-LHC beam intensity of 2.30×10^{11} p/b and at steady-state, this voltage corresponds to the present limit of the available (measured) rf power, with no operational margins left. If this injection voltage is needed to keep losses within acceptable limits, the power consumption at flat-bottom can thus become a bottleneck for the machine's future operation.

6. Future work

Start-of-ramp beam losses are the main limiting factor to determine the optimum (reduced) injection voltage, beneficial for rf power consumption and beam stability, since they directly impact machine

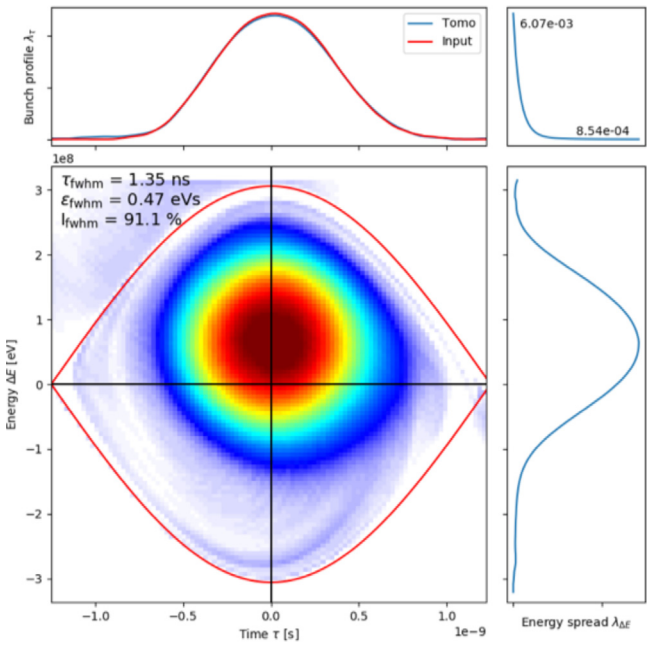

Fig. 10. Example of phase space tomography of a single bunch at LHC injection with a large energy error. The reconstruction was done using high-resolution profiles acquired at 40 MS/s, for 600 consecutive turns.

availability. Thresholds of acceptable beam losses in critical machine elements are being reevaluated by performing more accurate damage estimates.

The injection losses strongly depend on the SPS-LHC energy matching. Observations of beam injections with an energy mismatch twice as large as foreseen by the earlier SPS dipole field calibrations have highlighted the need for recalibration. Since the original LHC design, no dedicated work had been conducted on the SPS-LHC energy matching given that it had not posed any significant problem. Coupled with the tighter margins at the present lower voltage, these observations led to the current investigation of an improved SPS-LHC energy matching [30] which in turn will aid in reducing injection losses.

In the present observations, the energy mismatch measured through the dispersive orbit also showed systematic errors with respect to the optimally-matched values. A complementary measurement of energy and phase errors at injection can be done through phase space tomography [31,32], performed in the first few synchrotron periods after injection. An example of such a measurement is shown in Fig. 10. While this measurement was conducted only on demand in 2018, the studies presented in this paper triggered the implementation of an online machine-learning tomography, to be commissioned this year (2022). With this online tomography, it will be possible to measure batch-by-batch energy errors at injection. A reevaluation of the damping efficiency of injection errors and the power consumption of a longitudinal damper in the LHC is also planned.

Understanding capture losses and finding the minimum acceptable injection voltage in the LHC is the first step to assessing the rf power consumption for the HL-LHC. Tracking simulations modelling the dynamics of the beam and the cavity controller loops are ongoing [29]. Evaluating of the power consumption at injection, where it is expected to be the largest due to strong transient beam-loading, is challenging as it depends on the mismatch between the realistic SPS bunches and the capturing LHC buckets and the SPS-LHC energy shift at beam transfer.

7. Conclusions

The injection voltage of the LHC was originally chosen to be larger than the matched voltage to accommodate for energy and phase errors at beam transfer and thus minimise capture losses. However, when the voltage is high and large injection energy and/or phase errors occur, undamped oscillations are observed for high-intensity bunches, which can then lead to losses during flat-bottom. The reduction of the injection voltage not only helps to dampen injection oscillations, but it also reduces the rf power consumption at injection, which may become critical for the operation in the HL-LHC era.

Beam measurements spanning a month where the LHC injection voltage was reduced from 6 MV to 4 MV in operation were analysed. In this range, the injection voltage is above the quasi-matched value to accommodate for large-emittance bunches transferred from the twice-as-long SPS bucket into the LHC bucket. With the same bunches arriving from the SPS, the filamented LHC bunch lengths become longer as the voltage is reduced. The satellite population, although slightly increased as the injection voltage decreased, remained well below the 1% limit required by the LHC experiments. In the cases where a large SPS-LHC energy mismatch is present, beam losses can increase up to 60% of the dump threshold with the reduced injection voltage. Since no correlation between the dispersive orbit and manual tune trims is observed, it is concluded that errors in the LHC dipole and quadrupole fields are unlikely to be the source of the energy mismatch between the two machines. Overall, no operational disadvantage or beam quality degradation was found by operating with a 4 MV injection voltage.

Although machine availability was not affected by the increased losses in 2018, this might change in the future, as more spread in bunch parameters and larger emittances are expected with the increasing bunch intensity throughout Run 3 and beyond. To ensure continued high machine availability with reduced injection voltages, studies to minimise power transients at injection, reevaluate dump thresholds for beam losses and investigate potential sources of energy variation in the SPS are ongoing. The efficiency and power consumption overhead of a longitudinal damper at LHC injection are also under study.

CRediT authorship contribution statement

L. Medina: Software, Formal analysis, Investigation, Data curation, Writing – original draft, Writing – review & editing, Visualization. **H. Timko:** Conceptualization, Methodology, Software, Investigation, Writing – original draft, Writing – review & editing, Supervision. **T. Argyropoulos:** Software, Investigation, Resources, Supervision. **E. Shaposhnikova:** Validation, Writing – review & editing. **B. Salvachua:** Investigation, Resources. **J. Wenninger:** Investigation, Resources, Validation, Writing – review & editing. **I. Karpov:** Investigation, Writing – review & editing. **P. Baudrenghien:** Validation. **M. Palm:** Investigation.

Declaration of competing interest

The authors declare that they have no known competing financial interests or personal relationships that could have appeared to influence the work reported in this paper.

Acknowledgements

We thank W. Höfle, F. Gerigk, and B. Goddard for their comments during the preparation of this manuscript. Research supported by the HL-LHC project.

References

[1] O.S. Brüning, P. Collier, P. Lebrun, S. Myers, R. Ostojic, J. Poole, P. Proudlock, LHC Design Report, in: CERN Yellow Reports: Monographs, CERN, Geneva, 2004, URL http://cds.cern.ch/record/782076.

[2] E. Shaposhnikova, Longitudinal beam parameters during acceleration in the LHC, Technical Report No. LHC-PROJECT-NOTE-242, CERN, Geneva, 2000, URL https://cds.cern.ch/record/691957.

[3] E. Shaposhnikova, Longitudinal stability of the LHC beam in the SPS, Technical Report No. SL-Note-2001-031-HRF, CERN, Geneva, Switzerland, 2001, URL https://cds.cern.ch/record/702666.

[4] H. Damerau, A. Findlay, S.S. Gilardoni, S. Hancock, RF manipulations for higher brightness LHC-type beams, in: Proceedings of the 4th International Particle Accelerator Conference (IPAC'13), Shanghai, China, 2013, pp. 2600–2602, URL https://accelconf.web.cern.ch/IPAC2013/papers/wepea044.pdf.

[5] R. Moore, V. Balbekov, A. Jansson, V. Lebedev, K.Y. Ng, V. Shiltsev, C.Y. Tan, Longitudinal bunch dynamics in the Tevatron, in: Proceedings of the 20th Particle Accelerator Conference (PAC'03), Portland, OR, USA, 2003, pp. 1751–1753, URL https://accelconf.web.cern.ch/p03/PAPERS/TPPB066.pdf, paper TPPB066.

[6] A. Burov, Dancing bunches as van Kampen modes, in: Proceedings of the 24th Particle Accelerator Conference (PAC'11), New York, NY, USA, 2011, pp. 94–96, URL https://accelconf.web.cern.ch/PAC2011/papers/moods4.pdf, paper MOODS4.

[7] I. Karpov, T. Argyropoulos, E. Shaposhnikova, Thresholds for loss of Landau damping in longitudinal plane, Phys. Rev. Accel. Beams 24 (2021) 011002, http://dx.doi.org/10.1103/PhysRevAccelBeams.24.011002, URL https://link.aps.org/doi/10.1103/PhysRevAccelBeams.24.011002.

[8] C.Y. Tan, A. Burov, Phase modulation of the bucket stops bunch oscillations at the Fermilab Tevatron, Phys. Rev. ST Accel. Beams 15 (2012) 044401, http://dx.doi.org/10.1103/PhysRevSTAB.15.044401, URL https://link.aps.org/doi/10.1103/PhysRevSTAB.15.044401.

[9] I. Karpov, S. Albright, T. Argyropoulos, P. Baudrenghien, E. Shaposhnikova, H. Timko, LHC MD 2042: Persistent injection oscillations, Technical Report No. CERN-ACC-NOTE-2018-0018, CERN, Geneva, Switzerland, 2018, URL https://cds.cern.ch/record/2306249.

[10] J.F. Esteban Müller, H. Timko, E. Shaposhnikova, LHC MD 652: coupled-bunch instability with smaller emittance (all HOMs), Technical Report No. CERN-ACC-NOTE-2017-0017, CERN, Geneva, Switzerland, 2017, URL https://cds.cern.ch/record/2257554.

[11] H. Timko, T. Argyropoulos, I. Karpov, E. Shaposhnikova, Beam instabilities after injection to the LHC, in: Proceedings of the 61st ICFA Advanced Beam Dynamics Workshop on High-Intensity and High-Brightness Hadron Beams (HB'18), Daejeon, Korea, 2018, pp. 163–167, http://dx.doi.org/10.18429/JACoW-HB2018-TUP1WA03, URL http://jacow.org/hb2018/papers/tup1wa03.pdf, paper TUP1WA03.

[12] L. Medina, T. Argyropoulos, P. Baudrenghien, O. Brunner, R. Calaga, I. Karpov, F. Peauger, E. Shaposhnikova, H. Timko, K. Turaj, LHC MD 3165: RF power limitations at flat bottom, Technical Report No. CERN-ACC-NOTE-2019-0030, CERN, Geneva, Switzerland, 2019, URL https://cds.cern.ch/record/2683350.

[13] D. Boussard, RF power requirements for a high intensity proton collider. Part I, in: Proceedings of the 1991 IEEE Particle Accelerator Conference, San Francisco, CA, USA, 1991, pp. 2447–2449, http://dx.doi.org/10.1109/PAC.1991.164995, URL https://cds.cern.ch/record/221476, CERN-SL-91-16-RFS.

[14] P. Baudrenghien, T. Mastoridis, Proposal for an RF roadmap towards ultimate intensity in the LHC, in: Proceedings of the 3rd International Particle Accelerator Conference (IPAC'12), New Orleans, LA, USA, 2012, pp. 154–156, URL https://accelconf.web.cern.ch/IPAC2012/papers/moppc015.pdf, paper MOPPC015.

[15] H. Timko, E. Shaposhnikova, K. Turaj, Estimated LHC RF system performance reach at injection during Run III and beyond, Technical Report No. CERN-ACC-NOTE-2019-0005, CERN, Geneva, Switzerland, 2018, URL https://cds.cern.ch/record/2659670.

[16] I. Karpov, P. Baudrenghien, L. Medina, H. Timko, Consequences of longitudinal coupled-bunch instability mitigation on power requirements during the HL-LHC filling, in: Proceedings of the of the ICFA Mini-Workshop on Mitigation of Coherent Beam Instabilities in Particle Accelerators, CERN, Geneva, 2020, pp. 312–317, http://dx.doi.org/10.23732/CYRCP-2020-009.312, URL https://cds.cern.ch/record/2752421.

[17] L. Medina, T. Argyropoulos, R. Calaga, H. Timko, Studies of longitudinal beam losses at LHC injection, in: Proceedings of the 12th International Particle Accelerator Conference (IPAC'21), Campinas, SP, Brazil, 2021, pp. 4164–4167, http://dx.doi.org/10.18429/JACoW-IPAC2021-THPAB199, URL https://jacow.org/ipac2021/papers/thpab199.pdf, paper THPAB199.

[18] L. Medina, T. Argyropoulos, P. Baudrenghien, H. Timko, Cavity control modelling for SPS-to-LHC beam transfer studies, in: Proceedings of the 12th International Particle Accelerator Conference (IPAC'21), Campinas, Brazil, 2021, http://dx.doi.org/10.18429/JACoW-IPAC2021-THPAB200, URL https://jacow.org/ipac2021/papers/thpab200.pdf, paper THPAB200.

[19] G. Arduini, C. Arimatera, T. Bohl, P. Collier, K. Cornelis, J. Wenninger, Energy calibration of the SPS at 450 GeV/c with proton and lead ion beams, Technical Report No. AB-Note-2003-014-OP, CERN, Geneva, 2003, URL https://cds.cern.ch/record/702743.

[20] J. Wenninger, SPS momentum calibration and stability in 2003, Technical Report No. AB-Note-2003-091-OP, CERN, Geneva, 2003, URL https://cds.cern.ch/record/702823.

[21] O.C. Brunner, H. Frischholz, D. Valuch, RF power generation in LHC, Technical Report No. LHC-Project-Report-648, CERN-LHC-Project-Report-648, CERN, Geneva, 2003, URL https://cds.cern.ch/record/620365.

[22] T. Mastoridis, P. Baudrenghien, J. Molendijk, Cavity voltage phase modulation to reduce the high-luminosity Large Hadron Collider rf power requirements, Phys. Rev. Accel. Beams 20 (2017) 101003, http://dx.doi.org/10.1103/PhysRevAccelBeams.20.101003, URL https://link.aps.org/doi/10.1103/PhysRevAccelBeams.20.101003.

[23] CERN BLonD Simulation Suite, 2022, URL http://blond.web.cern.ch.

[24] H. Timko, S. Albright, T. Argyropoulos, K. Iliakis, I. Karpov, A. Lasheen, L. Medina, D. Quartullo, J. Repond, J. Esteban Müller, M. Schwarz, P. Tsapatsaris, BEam Longitudinal Dynamics Simulation Suite blond, 2022, arXiv preprint arXiv:2206.08148, http://dx.doi.org/10.48550/ARXIV.2206.08148.

[25] B. Dehning, The LHC beam loss measurement system, in: Proceedings of the 22nd Particle Accelerator Conference (PAC'07), Albuquerque, NM, USA, 2007, pp. 4192–4194, URL https://cds.cern.ch/record/1057235/files/lhc-project-report-1025.pdf, paper FRPMN071.

[26] B. Dehning, Beam Loss Monitors at LHC, CERN Yellow Reports, 2, 2016, p. 303, http://dx.doi.org/10.5170/CERN-2016-002.303, URL https://e-publishing.cern.ch/index.php/CYR/article/view/238.

[27] M. Palm, E. Bravin, S. Mazzoni, Near-saturation single-photon avalanche diode afterpulse and sensitivity correction scheme for the LHC longitudinal density monitor, in: Proceedings of the 3rd International Beam Instrumentation Conference (IBIC'14), Monterey, CA, USA, 2014, pp. 169–173, URL http://jacow.org/IBIC2014/papers/mopd11.pdf, paper MOPD11.

[28] P. Baudrenghien, G. Hagmann, J. Molendijk, R. Olsen, A. Rohlev, V. Rossi, D. Stellfeld, D. Valuch, U. Wehrle, The LHC Low Level RF, Technical Report No. LHC-PROJECT-Report-906, CERN, Geneva, 2006, URL https://cds.cern.ch/record/971742.

[29] H. Timko, Status of the LHC injection voltage limits with half-detuning, 2019, Talk at the 9th HL-LHC Collaboration Meeting, Fermilab, Chicago, US, URL https://indico.cern.ch/event/806637/contributions/3573670/.

[30] V. Kain, T. Argyropoulos, K. Li, J. Wenninger, SPS-LHC energy matching – update, 2020, Talk at the LIU-SPS Coordination Meeting, CERN, Geneva, Switzerland, URL https://indico.cern.ch/event/977192/contributions/4115701/.

[31] S. Hancock, A simple algorithm for longitudinal phase space tomography, Technical Report No. CERN-PS-RF-NOTE-97-06, CERN, Geneva, 1997, URL https://cds.cern.ch/record/1174559.

[32] S. Hancock, J.-L. Sanchez Alvarez, A pedestrian guide to online phase space tomography in the CERN complex, Technical Report No. CERN-PS-RF-NOTE-2001-010, CERN, Geneva, 2001, URL https://cds.cern.ch/record/960231.